

# Density Measurements During Ion Cyclotron Heating in VASIMR

Christopher N. Davis\* and Brian E. Gilchrist†  
*University of Michigan, Ann Arbor, MI, 48109*

Jared P. Squire‡  
*Advanced Space Propulsion Laboratory, JSC/NASA, Houston, TX*

and

Franklin R. Chang Diaz§  
*Advanced Space Propulsion Laboratory, JSC/NASA, Houston, TX*

The response of ions during single-pass ion cyclotron resonance heating can be nonlinear [1]. The ion flow is accelerated due to the gradient along the axial magnetic field, and the electric and magnetic fields of the cyclotron-heating wave. This acceleration will produce a decrease in the plasma density around the resonance point depending on the incident flow velocity and the amount of power that is coupled into the ions at the resonance frequency. The primary application of this work is the acceleration of ions for electric propulsion systems. The experimental work for this paper was done on the Variable Specific Impulse Magnetoplasma Rocket (VASIMR) that is being developed by Johnson Space Center. The measurements were taken using a 70 GHz density interferometer system. Density measurements taken during ion cyclotron heating show a clear and repeatable density drop of about 25% for Helium plasma and about 75% for Deuterium plasma. Initial calculations also show that the measured results agree well with theory.

## Nomenclature

$\omega_{LH}$	=	lower hybrid frequency
$\omega_{ce}$	=	electron gyrofrequency
$\omega_{pe}$	=	electron plasma frequency
$M_i$	=	ion mass
$M_e$	=	electron mass
$q$	=	ion charge
$e$	=	electron charge
$B$	=	RF magnetic field vector
$B_o$	=	DC magnetic field vector
$E$	=	electric field vector
$V$	=	velocity vector
$n$	=	electron density
$c$	=	speed of light
$\omega$	=	angular frequency
$A$	=	Amplitude
$k$	=	wave vector

---

\* Graduate Student Research Assistant, Electrical Engineering and Computer Science, AIAA member

† Professor and Associate Chair, Electrical Engineering and Computer Science; Professor, Atmospheric, Oceanic, and Space Sciences, AIAA member

‡ Senior Research Scientist, Muniz Engineering, Inc. AIAA member

§ NASA Astronaut, ASPL Director, AIAA member.

- $z$  = axial component\*
- $+$  = combined perpendicular component (with respect to  $z$ )\*
- $x,y$  = x or y component\*
- $T_e$  = electron temperature
- ICRH = ion cyclotron resonance heating
- $\theta_o$  = phase offset
- $L$  = scale length of axial DC magnetic field
- $L_p$  = plasma path length
- $\phi_p$  = phase shift through plasma
- $V_{off}$  = DC voltage offset
- $u$  = magnetic moment

\*Vectors with these subscripts represent that particular component of the vector

### I. Introduction

The Variable Specific Impulse Magnetoplasma Rocket (VASIMR) is a next generation ion engine being developed at the Advanced Space Propulsion Lab (ASPL) located at NASA's Johnson Space Center. VASIMR is a high power magnetoplasma rocket, capable of ISP/thrust modulation. The overall design focus behind the VASIMR project has been to develop a space engine capable of flying a human mission to Mars. For human missions, spacecraft must possess some key features, which are not necessarily critical for robotic missions. Human vehicles must be fast, reliable, "power rich", and be capable of abort options for crew survival in the event of unexpected malfunctions. [5]

Research on the VASIMR engine started in the late 1970's from an offshoot on fusion technology research of magnetic drivers [5]. These studies were motivated by the intriguing properties of expanding magnetoplasma jets and their potential application to power generation and advanced propulsion. The diagram below shows the basic layout of the VASIMR concept.

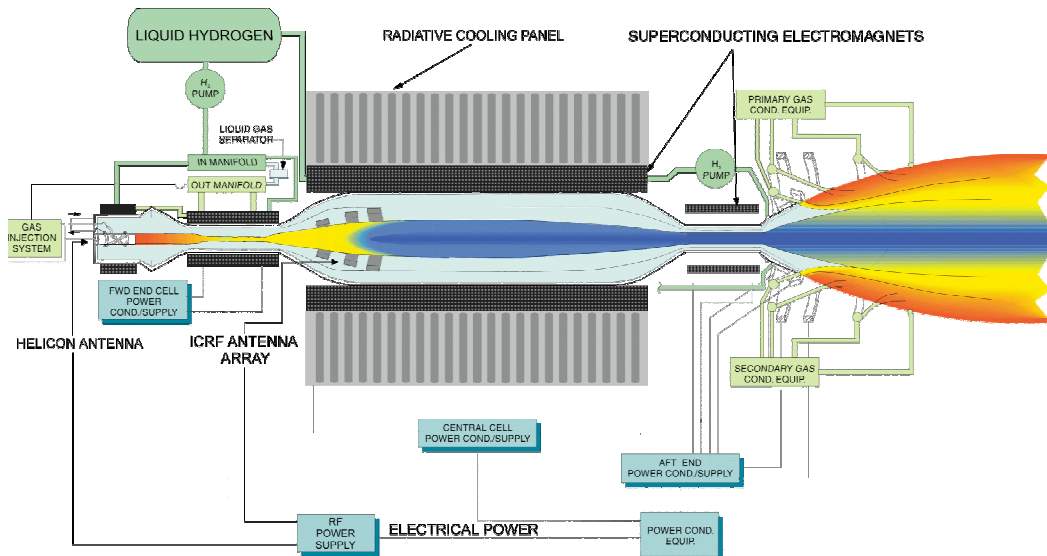


Figure 1. Schematic of the VASIMR Concept

The engine consists of 3 sections. The forward section is where the injection of the propellant gas and its ionization is done. The middle section amplifies or heats the plasma. And the aft cell converts the energy of the plasma into a directed flow using a magnetic nozzle.

## A. Basic Physics of Operation

### 1. Forward Section

In the forward most stage, a cold and dense plasma is produced by ionizing a gas (in most cases Helium or Deuterium) using a helicon. Helicons are propagating wave modes in a finite axially magnetized plasma column. The electric and magnetic fields of the modes have radial, axial, and usually, azimuthal variation [2]. They propagate in a low frequency compared to the electron plasma frequency, low magnetic field regime, and high density regime characterized by

$$\omega_{ci} \ll \omega \ll \omega_{ce}$$

$$\omega_{pe}^2 \gg \omega \omega_{ce}$$

where  $\omega_{LH}$  is the lower hybrid frequency, and  $\omega_{ce}, \omega_{pe}$  the electron gyrofrequency and plasma frequency, respectively. The driving frequencies for helicon waves is typically 1-50 MHz, the DC magnetic field about 0.02 - 0.2 T, and the densities on the order of  $10^{11}$ - $10^{14}$  cm<sup>-3</sup>. Typical operating conditions for the VASIMR experiment at ASPL are 0.18 T DC magnetic field, 20 MHz helicon frequency, and densities in the area of  $10^{13}$  cm<sup>-3</sup>.

### 2. Central Section

After plasma creation by the helicon source, the charged particles then flow along the field lines down to the central section of the engine where they are heated by a process known as ion cyclotron resonance heating (ICRH).

The Lorentz force on the particles in the presence of a magnetic field forces them to follow circular paths

characterized by the Larmor radius and the cyclotron frequency, given by the equations  $r_L = \frac{M_i v_{\perp}}{q B_0}$  for the Larmor

radius and  $\omega_i = \frac{q B_0}{M_i}$  for the ion cyclotron frequency where  $M_i$  is the mass of the ion,  $q$  is the charge of the ion,

and  $B_0$  is DC magnetic field. The Larmor radius represents the radius of the circular path the particles are following and the Larmor frequency represents the number of times the particles rotate around per second.

Ion cyclotron resonance heating (ICRH) is a plasma heating technique in which RF energy is coupled into the plasma at the same frequency that the ions are rotating within the magnetic field. ICRH is discussed in more detail in the following section.

### 3. Aft Section

In this section of VASIMR the perpendicular energy of the ions generated by ICRH is converted into axial energy by the decreasing gradient of the axial magnetic field from conservation of the magnet moment. The aft section is also the region where detachment of the plasma from the magnetic field takes place. The detachment of the plasma from the field takes place largely due to the loss of adiabaticity and the rapid increase of the plasma  $\beta$  which is the ratio of the plasma pressure to the magnetic pressure. This section is usually referred to as the magnetic nozzle.

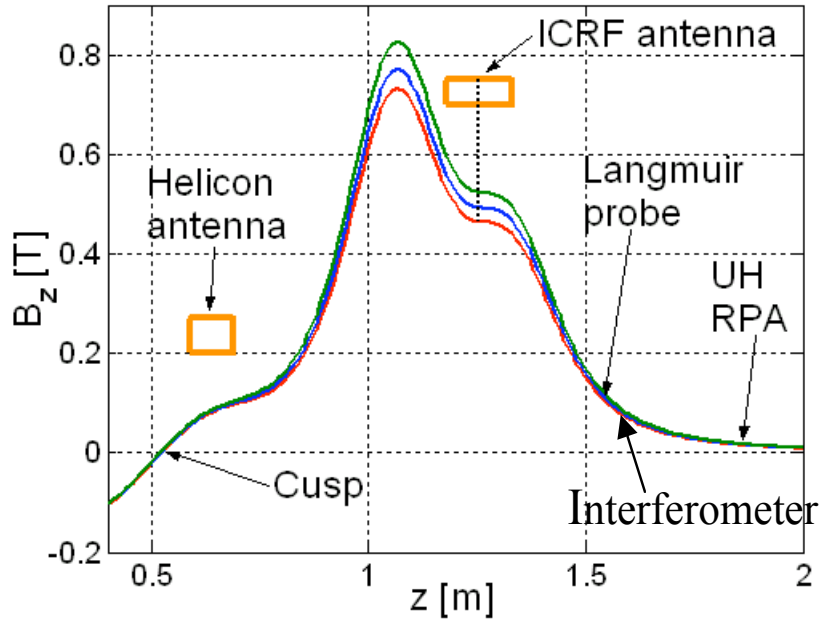


Figure 2. Typical Axial Magnetic field profile in the VASIMR Experiment

A laboratory version of a 25 kW proof of concept VASIMR engine, the VX-10, has been under development and test at the Advanced Space Propulsion Laboratory (ASPL) at Johnson Space Center. All experimental work described below was performed on this system. Figure 2 shows a typical axial magnetic field profile used during operation. See figure 6 for a schematic of the VX-10.

## II. ICRH Theory

As mentioned previously, the VASIMR concept employs an ion-cyclotron-resonance-heating (ICRH) as the method for heating the plasma. The source creates plasma that flows along the field lines down the magnetic field gradient towards the ICRH section. Once in the ICRH section there will eventually be a point where the ion gyro-frequency will match the frequency being supplied by the RF heating antenna, which will give efficient coupling into the ion gyro-motion causing the ions to heat up (i.e a transfer of RF energy into rotational energy).[1],[4]

The ICRH in VASIMR has two properties

- (1) Each ion passes the resonance only once
- (2) The ion motion is collisionless

This means that the ion final energy should depend only on the incident-flow velocity. This can be broken up into two cases.

- (1) The ion is traveling fast enough so that its velocity does not change significantly at the resonance point. Which means that the ion density is fairly constant at the resonance point. This is essentially a linear problem and as will be shown gives 100% absorption of the RF energy.
- (2) The ions are moving slow enough so that they can be significantly accelerated along the magnetic field. The forces responsible for their acceleration are the force due the magnetic field gradient and the rf-pressure. This makes the problem non-linear and can produce a steep decrease in the plasma density at the resonance point.

### A. General Theory Near the Resonance Point

The following assumptions are made in the plasma

- (1) Collisionless
- (2)  $B_{oz} \gg B_{or}$ ,

- (3) The magnetic field decreases monotonically along z

The ICRH RF wave has a direction of propagation that is nearly parallel to the magnetic field lines. The location of the resonance point is defined as  $z = 0$  and a linear approximation for the ion gyro-frequency near the resonance is used

$$\omega_{ci} = \omega(1 - z/L) \quad (1)$$

To find the ion velocity ( $V_x, V_y$ ), the ion momentum balance equation is used. The following assumptions are made to simplify the equation.

- (1) The x and y derivatives of the RF electric and magnetic fields are small near the resonance
- (2)  $E_z = 0$  because of the high conductivity of the electrons
- (3)  $n, V_z$  are time independent

Combining equation (1) with the momentum balance equations and using the above assumptions, the equation for  $V_x$  and  $V_y$  components of the ion velocity can be found

$$\frac{\partial V_x}{\partial t} + V_z \frac{\partial V_x}{\partial z} = \frac{eE_x}{m_i} + \omega(1 - z/L)V_y \quad (2)$$

$$\frac{\partial V_y}{\partial t} + V_z \frac{\partial V_y}{\partial z} = \frac{eE_y}{m_i} + \omega(1 - z/L)V_x \quad (3)$$

The spatial dependence of  $V_z$  (it is time independent) is determined by the momentum balance equation along z.

$$m_i V_z \frac{\partial V_z}{\partial z} = -u \frac{\partial B_{oz}}{\partial z} + q \langle V_x B_y - V_y B_x \rangle - m_i \frac{T_e}{m_i} \frac{1}{n} \frac{\partial n}{\partial z} \quad (4)$$

The three terms on the right hand side of the equations represent the following in order of left to right.

- (1) The force of the ion due to the gradient of the magnetic field
- (2) The z component of the Lorentz force equation from the RF wave (RF pressure)
- (3) The force associated with the ambipolar electric field.

The brackets in (4) represent an averaging of the RF pressure force over several ion gyrations.

Assuming the polarization of the incoming wave is circular, the electric field as well as the x,y components of the magnetic field and ion velocity have the following form

$$A_x = \frac{1}{2} A_+(z) e^{-i\omega t} \quad (5)$$

$$A_y = \frac{1}{2} A_+(z) e^{-i(\omega t + \pi/2)} \quad (6)$$

where  $A = E, B$  or  $V$  for electric field, magnetic field or ion velocity, respectively and  $A_+(z)$  is a complex amplitude. Using all of the above equations/assumptions, and Maxwell equations, the following closed set of equations for  $E_+, B_+, V_+, V_z$ , and  $n$  can be defined.  $E_+, B_+, V_+$  in the equations below are the complex amplitudes of the RF electric and magnetic fields and the perpendicular velocity. The velocity,  $V_+$ , represents the cyclotron velocity of the ions.

$$V_z \frac{\partial V_z}{\partial z} = \frac{|V_+|^2}{2L} - \frac{1}{8\pi m_i n} \frac{\partial |B_+|^2}{\partial z} - \frac{c_s^2}{n} \frac{\partial n}{\partial z} \quad (7)$$

$$V_z \frac{\partial V_+}{\partial z} = \frac{e}{m_i} E_+ + i\omega \frac{z}{L} V_+ \quad (8)$$

$$j = nV_z = \text{const.} \quad (9)$$

Equation (7) is the axial momentum balance equation for the ions where  $u$  is the magnetic moment and Equation (8) is the transverse momentum balance equation. Equation (9) is the continuity of current within the plasma.

### B. Non-Linear Resonance

The absorption of the heating wave to ion motion is 100% as long as the ion velocity in the  $z$  direction is approximately constant or the resonance area extends over several wavelengths. If the RF power is high enough or the ion velocity ( $V_z$ ) is slow enough, then axial forces due to the RF wave and magnetic gradient will create a density gradient in the resonance area.

When this happens, not all of the energy is converted into plasma motion by the RF heating wave. Since the ions are unable to carry away all of the energy of the incoming wave, part of the energy must go into a reflected wave. Another way to understand the reflection is that the ion density exhibits a steep drop in the non-linear region, which happens over a distance that is shorter than the RF wavelength.

VASIMR operates in the non-linear region of ICRH. The primary cause of non-linearity (non-constant  $V_z$ ) is the force placed on the ions due to the magnetic field gradient. From conservation of current through the resonance zone (9), the ion (and therefore electron) density must decrease as  $V_z$  increases. Figure 3 shows the density solved as a function of axial position ( $z$ ) using equations (7)-(9). In equation (7), all but the first term on the right-hand-side was ignored. [1] The RF electric field was assumed to be constant throughout the resonance zone. The  $z=0$  is defined as the point where the RF wave frequency is equal to the ion cyclotron frequency. Positive values of  $z$  are downstream of the resonance and negative values of  $z$  are upstream. It can be seen that the density gradient gets less pronounced as the ions enter the resonance zone at a faster velocity. The densities were normalized by multiplying through by the initial axial velocity.

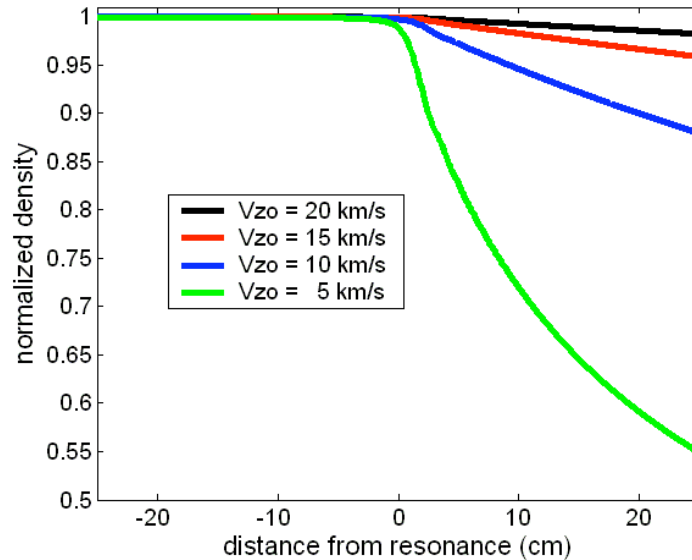


Figure 3. Calculated Density Profiles for Increasing Ion Axial Velocity during ion cyclotron heating

### III. Interferometer Description

A 70 GHz interferometer system has been installed on the VX-10 device and was the primary measurement device used. A significant advantage of a millimeter wave interferometer over other diagnostics is it allows a non-intrusive method of measuring plasma density. The design was based on a similar interferometer at UCLA [8].

#### A. Interferometer Theory

The dispersion relationship of an electromagnetic wave propagating in plasma where the cyclotron frequency is much smaller than the wave frequency or the propagating wave is parallel to the DC field is given below.

$$\frac{c^2 k^2}{\omega^2} = 1 - \frac{\omega_{pe}^2}{\omega^2} \quad (10)$$

This shows that the propagation vector for the wave is dependent on electron density. The net phase shift of a wave through a plasma compared to free space can then be calculated as follows

$$\Delta\theta(t) = \int_{-L/2}^{L/2} [k_o - k_p(x,t)] dx \quad \text{with} \quad k_p = k_o \sqrt{1 - \frac{f_p^2}{f^2}}, \quad f_p^2 = \frac{n(x,t)e^2}{4\pi^2 \epsilon_o m_e} \quad (11)$$

If  $f > 3f_p$ , where  $f$  is the frequency of the wave and  $f_p$  is the plasma frequency, then the expression above can be simplified by expanding the expression for  $k_p$  in a Taylor series and keeping only the first two terms. Giving the following

$$\Delta\theta(t) = \frac{e^2}{4\pi\epsilon_o m_e c f} \int_{-L_p/2}^{L_p/2} n(x,t) dx \quad (12)$$

The term  $\int_{-L_p/2}^{L_p/2} n(x,t) dx$  is commonly referred to as the line integrated density or total electron content (TEC).

It represents a summation of the plasma density over the particular path that the wave is traveling and is proportional to the phase shift. If a specific density spatial distribution is assumed then the term above can be integrated and the actual density can be found as a function of position.

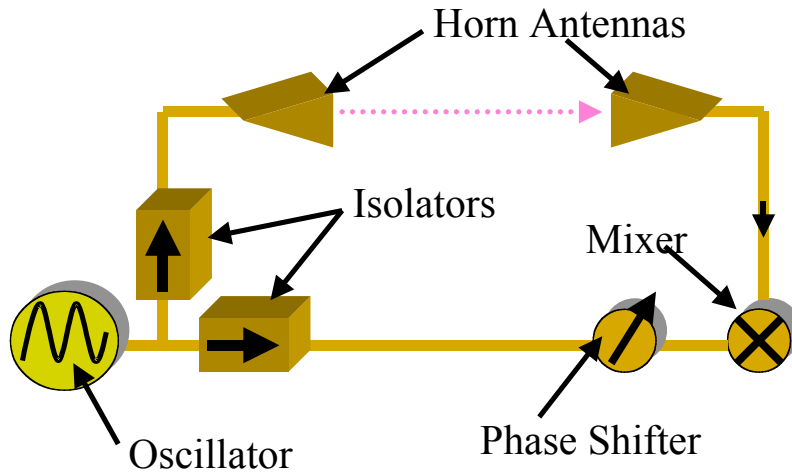
#### B. System Operation

Figure 4 shows a layout of the setup of the interferometer. The basic operation of the system is as follows. The oscillator generates 15 dBm of power at 70 GHz. The signal is then split by a 3 dB coupler sending part of the signal to the antennas to be transmitted through the plasma, and the other part to the local oscillator power for the mixer. Since the mixer are mixing two signals that are of the same frequency, the IF output of the mixer has the following form

$$V(t) = A \cos(\phi_p(t) + \theta_o) + V_{off} \quad (13)$$

where  $\phi_p$  is the net phase shift through the plasma,  $\theta_o$  is the phase offset from 0 degrees,  $V_{off}$  is the DC voltage offset of the mixers from zero, and  $A$  is the amplitude of the voltage swing of the mixers. Adjusting the phase shifter shown in the system diagram can vary  $\theta_o$ . The isolators were put in to protect the oscillator from power reflections. It was also necessary to magnetically shield the isolators from the high ambient magnetic field. Without the magnetic shielding it was found that the magnetic field changed the voltage output of the mixers even without plasma present.

The antennas are 25 dB gain horn antennas. The 3dB beamwidth of the horns is about 10 degrees giving a spot size on the plasma of about 6 cm in diameter and a spot size of about 12 cm on the opposite port of the chamber.



**Figure 4. Diagram of the Interferometer System Installed on the VX-10 Experiment**

During measurements the phase shifter is adjusted so that  $\theta_o$  is approximately equal to 90 degrees. The data collection system on the VX-10 begins to measure the interferometer signal a short time before the plasma comes on. By taking the difference between the interferometer signal with the plasma on and off, the offset term can be cancelled out. The main source of error in the measurements was found to be the drift of the Amplitude term (A) in equation (13). This was compensated for somewhat by applying temperature control to the oscillator. The current error of the system is estimated to be about 10%. The actual density (as opposed to line integrated) was found by using the density profile measured by the reciprocating langmuir probes and scaling it based on the magnetic field to the location of the interferometer allowing equation (12) to be solved directly. Figure 5 shows a sample shot of the interferometer measurements.

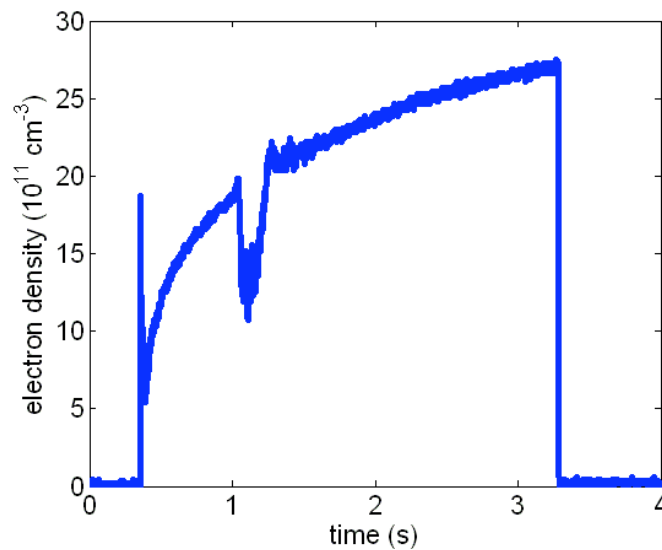


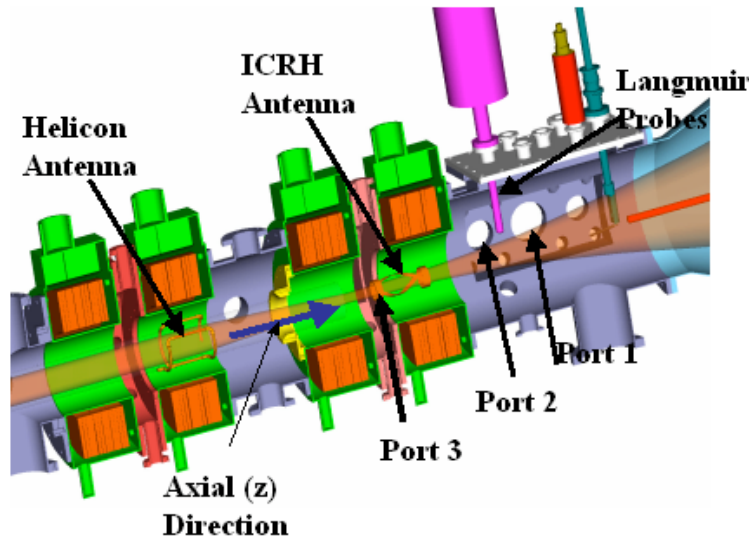
**Figure 5. A sample shot of processed interferometer data for He at 9 kW of Helicon Power**



The dip in density is when the langmuir probes are fired. The steady rise in density throughout the length of the plasma pulse is most likely due to collisions with neutrals slowing the flow. The peak density measured by the probes agrees well with the interferometer data at about  $2 \times 10^{12} \text{ cm}^{-3}$ .

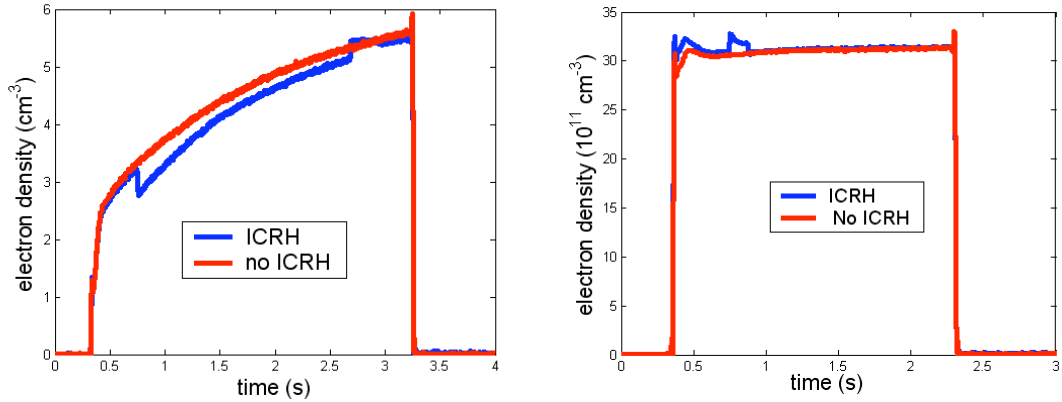
#### IV. Experimental Results

Interferometer measurements were taken at three locations on the VX-10 experiment labeled for the purposes of this paper as port 1, port 2, and port 3. Port 1 and 2 are located well downstream of the Ion cyclotron resonance and port 3 is located directly underneath the ICRH antenna. Figure 6 shows the locations. Axial position ( $z$ ) refers to the axial direction along the VX-10 experiment as is shown in the figure. Increasing  $z$  represents moving further down stream in the experiment. The perpendicular direction is defined as the two directions ( $x,y$ ) perpendicular to the  $z$  direction.



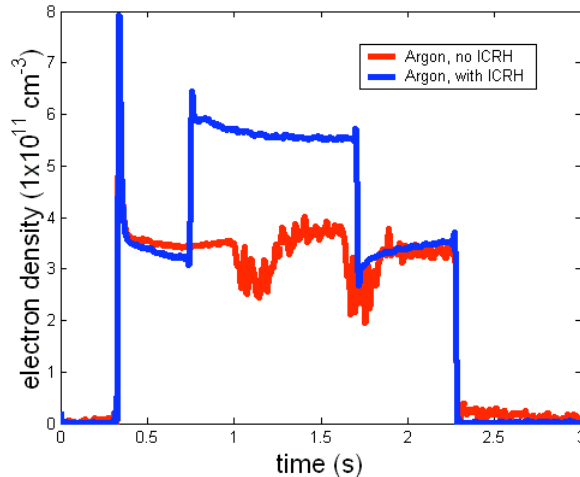
**Figure 6. Interferometer Measurement Locations on the VX-10 Experiment**

Figure 7 shows typical examples of density measurements taken downstream (left figure) and upstream (right figure) of the resonance location for Helium at a flow rate of 110 sccm. ICRH power comes on for a fraction of the time of the total plasma pulse. (It should be noted that the down stream ICRH pulse length was longer than the upstream.) The plasma density consistently decreased about 20-30% downstream and increased about 5% upstream of resonance. This indicates that the plasma is being accelerated as it moves down the magnetic field gradient.



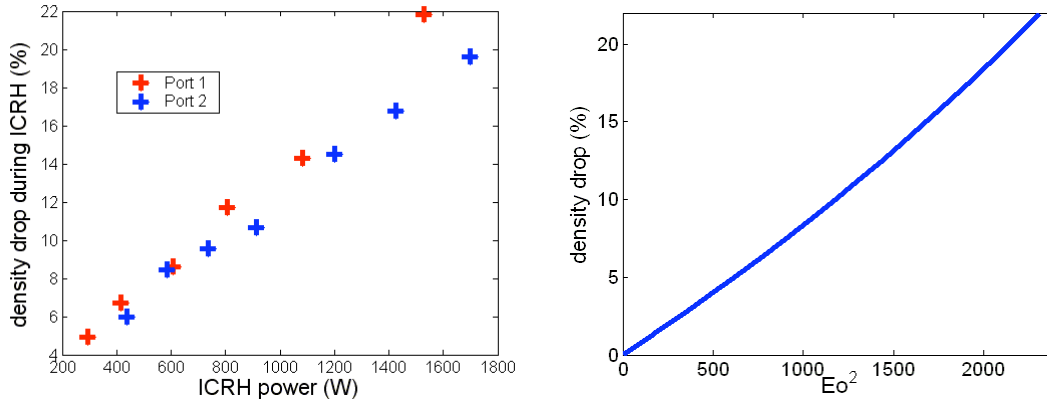
**Figure 7. Density measured during an ICRH pulse downstream (port 1) and upstream (port 3) on the VX-10 experiment**

Figure 8 shows density measurements taken at port 1 using Argon gas instead of Helium, but using an ICRH frequency in the Helium range (1.8 MHz) so that there is no resonance point for the magnetic field values in the experiment. As can be seen from the figure, the density increases downstream indicating that the ICRH energy is creating plasma, as opposed to accelerating it as with Helium.



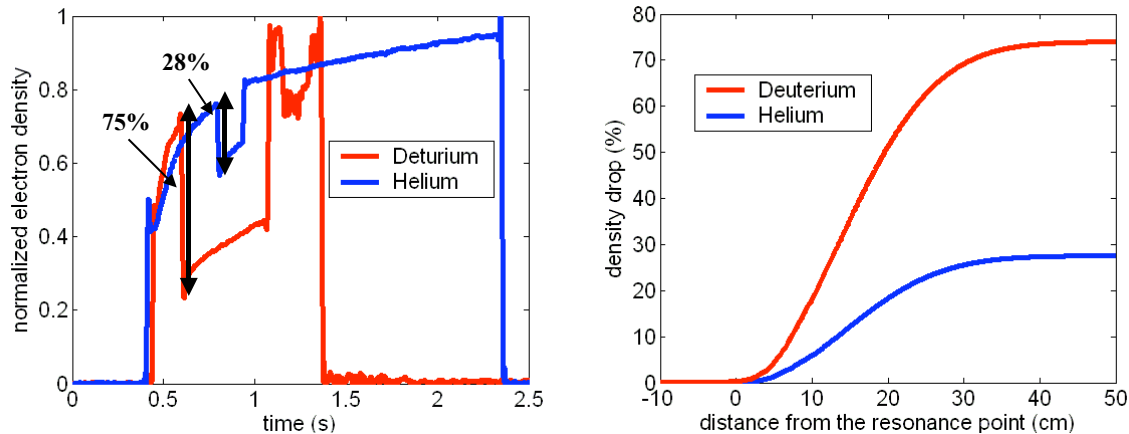
**Figure 8. Density measured during an ICRH pulse downstream (port 1) on the VX-10 with Argon**

Figure 9 on the left side shows the measured density drop at port 1 and port 2 for Helium as ICRH power is increased. The density drop is defined as the value of the density right before the ICRH power turns on subtracted from the density value after divided by the density before ICRH turns on. The right side of Figure 9 shows the calculated density based on equations (7)-(9). The magnetic field profile used was similar to the one shown in figure 2 and the initial axial velocity ( $V_z$ ) was assumed to be 15 km/s based on experimental results [6]. The initial perpendicular velocity ( $V_+$ ) was set to 0. As can be seen from the figure, the shape of the curve matches well with what was observed.



**Figure 9. Predicted density drop versus measured density drop during ICRH as a function of Power**

Figure 10 on the left side shows the measured density drop taken at port 1 for Deuterium and Helium gas. The density drop was measured to be about 28% for Helium and 75% for Deuterium for the same value of ICRH power and similar operating conditions. It should be noted the magnetic field in the experiment is scaled by one half so the same frequency can be used in the ICRH for Helium and Deuterium. The right hand side of figure 10 shows the calculated density drop as a function of axial position using equations (7)-(9). The initial axial velocity was set to 15 km/s. The only difference in the calculation between He and D2 was scaling the field profile and ion mass of the Deuterium case by a factor of 2. The final downstream density drop calculated is similar in both cases to what was measured.



**Figure 10. Calculated versus Measured Density drop for Deuterium and Helium during Ion Cyclotron Heating**

## V. Conclusion

The use of ion cyclotron heating for the acceleration of ions as described is a new concept in electric propulsion. These measurements are part of the first work in this area to experimentally characterize and analyze such a process. This work will help to lay the foundation for understanding the key parameters in ion cyclotron acceleration and to evaluate its feasibility as a method for space propulsion.

## Acknowledgments

The research was funded by NASA L. B. Johnson Space Center and through the NASA GSRP program. Authors C. Davis and Dr. B. Gilchrist would like to thank the ASPL team for all their help and support that made this work possible.

## References

- [1] Breizman B. N., Arefiev A. V. (2001), *Single-Pass Ion Cyclotron Resonance Absorption*, Physics of Plasmas, **8** (3) 907-915, 2001
- [2] Lieberman , **Principles of Plasma Discharges and Materials Processing**, 1994
- [3] Budden, **Radio Waves in the Ionosphere**, 1966
- [4] Stix, **Theory of Plasma Waves**, 1962
- [5] Chang Díaz F. R. (2002), *The VASIMR Engine: Concept Development, Recent Accomplishments and Future Plans*, Open Systems, July 1-5, 2002, Jeju Island, Korea, Transactions of Fusion Technology.
- [6] Squire J. P., Chang Díaz F. R., Glover T. W., Jacobson V. T., Chavers D. G., Bengtson R. D., Bering E. A. III, Boswell R. W., Goulding R. H., Light M. (2002), *Progress in Experimental Research of the VASIMR Engine*, Open Systems, July 1-5, 2002, Jeju Island, Korea, Transactions of Fusion Technology.
- [7] Ilin A. V., Chang Díaz F. R., Squire J. P., Carter M. D. (2002), *Radio Frequency Field Calculations for Plasma Heating Simulations in VASIMR*, IAC-02-S.P.07, 53rd International Astronautical Congress / The World Space Congress, October 10-19, 2002, Houston, TX.
- [8] M. Gilmore, W. Gekelman, K. Reiling, and W.A. Peebles, **A Reliable Millimeter Wave Quadrature Interferometer**, Institute of Plasma and Fusion Research, University of California, Los Angeles, California 90024, <http://128.97.43.7/lapd/General/Diagnostics/Interferometer/reliable.html>
- [9] **Design of High-Density Sources for Materials Processing**, "Physics of Thin Films", Vol. 18 by Academic Press, Inc., Publisher in Press
- [10] M. D. Carter, F. W. Baity, G. C. Barber, and R. H. Goulding, **Comparing experiments with modeling for light ion helicon plasma sources**, Physics of Plasmas, Volume 9, Number 12.